Light-Dressing Effect in Laser-Assisted Elastic Electron Scattering by Xe

Yuya Morimoto, Reika Kanya, and Kaoru Yamanouchi*
Department of Chemistry, School of Science, The University of Tokyo, 7-3-1, Hongo, Bunkyo-ku, Tokyo 113-0033, Japan
(Received 26 February 2015; published 16 September 2015)

The light-dressing effect in Xe atoms was identified in laser-assisted elastic electron scattering (LAES) signals. In the angular distribution of LAES signals with energy shifts of $\pm\hbar\omega$ recorded by the scattering of 1 keV electrons by Xe in an intense nonresonant laser field, a peak profile appeared at small scattering angles (<0.5°). This peak was interpreted as evidence of the light dressing of Xe atoms induced by an intense laser field on the basis of a numerical simulation in which the light-dressing effect is included.

DOI: 10.1103/PhysRevLett.115.123201 PACS numbers: 34.80.Qb

When an electron is elastically scattered by an atom in a laser field, the kinetic energy of the scattered electron changes by multiples of photon energy $n\hbar\omega$, where n is an integer ($n = 0, \pm1, \pm2\ldots$) and ω is an angular frequency of the laser field [1–3]. This scattering process is called laser-assisted elastic electron scattering (LAES). The LAES process is intuitively described as follows. The trajectory of the projectile electron approaching the target atom is modulated by the interaction between the laser field and the projectile electron. Then, during the collision process, the projectile electron interacts with the target atom, electrons of which are quivered by the laser-atom interaction. Finally, the resultant scattered electron is modulated again by the laser-electron interaction. Therefore, three kinds of interactions, i.e., the laser-electron interaction, the electron-atom interaction, and the laser-atom interaction, coexist in the LAES process, leading to intriguing changes in the energy and angular distributions of the scattered electrons. Regarded as a phenomenon that has fundamental importance in collision physics, the LAES process has long been studied both experimentally [4] and theoretically [5].

In 1973, Kroll and Watson derived a formula for the differential cross section of the LAES process when the laser-atom interaction can be neglected [6]. Within the framework of the Kroll-Watson approximation, the information that can be obtained on the target atom from the differential cross section of the LAES process is the same as that obtained from the differential cross section of elastic scattering without laser fields (see the Supplemental Material [7]). When the laser field is strong and/or its frequency is near the resonance frequency of an optical transition of the target atom, the spatial distribution of electrons in the target atom is distorted through the strong laser-atom interaction. Consequently, the energy and angular distributions of the scattered electrons in the LAES process are varied in response to the spatiotemporal changes in the electron density distribution of the target atom. This light-dressing effect in the LAES process was first discussed by Gersten and Mittleman in 1976 [8], and has been an attractive issue in theoretical studies for more than three decades [3]. In 1984, Byron and Joachain obtained the differential cross section of the LAES process with the energy shift (ΔE) of $n\hbar\omega$ ($n = 0, \pm1$) by adopting the first-order time-dependent perturbation theory to the laser-atom interaction [9]. They showed that an intense peak structure appears at small scattering angles in the differential cross sections of the LAES processes with one-photon energy shifts ($\Delta E = \pm\hbar\omega$). The peak profile appearing in the small scattering angles was also reported by Dubois *et al.* [10] and Dörr *et al.* [11]. These theoretical studies showed that small-angle LAES signals carry valuable information on the electron density distribution in a target atom influenced by an external laser field, which will be of use in understanding dynamics of electrons in the attosecond time domain [12] and strong-field induced molecular processes [13].

On the other hand, the light-dressing effect in target atoms has not been confirmed experimentally. Since the pioneering experiments of Andrick and Langhans in 1976 [14] and Weingartshofer *et al.* in 1977 [15], most of the LAES experiments have been conducted using cw and pulsed-CO_2 lasers [4]. Because the wavelength of the CO_2 lasers ($\lambda = 10.6\ \mu$m) is considerably longer than resonance wavelengths of optical transitions of atoms and the laser field intensities are relatively moderate ($\leq 10^9$ W/cm^2), the results of the conventional LAES experiments were well reproduced by the simulation based on the Kroll-Watson approximation, in which the laser-atom interaction is neglected. The only exceptions were the results reported by Wallbank and Holmes [16–19] and Musa *et al.* [20]. They observed unexpectedly large differential cross sections at specific scattering angles where the Kroll-Watson approximation predicts almost zero cross sections. Theoretical studies [21–27] showed that the light-dressing effects in the Wallbank and Holmes's experimental conditions are too small to account for the discrepancies, and several theoretical studies [27–33] suggested that the double scattering is a possible cause of the discrepancies. The result of Musa *et al.* has not been discussed theoretically, and therefore, the origin of the discrepancies in their case has not been explored yet.

 © 2015 American Physical Society

More recently, deHarak *et al.* [34,35] reported the LAES signals induced by near-infrared laser pulses with moderate intensities ($I \sim 5 \times 10^9$ W/cm^2, $\lambda = 1064$ nm), and confirmed that the LAES signals in their experimental conditions are consistent with the Kroll-Watson approximation [34,35]. In our recent study [36], we conducted LAES experiment within the scattering angle (θ) range of $2° \leq \theta \leq 14°$ in the near-infrared region ($\lambda = 800$ nm) with the high laser field intensity ($I = 1.8 \times 10^{12}$ W/cm^2), which is more than 3 orders of magnitude larger than the laser field intensities in the previous LAES experiments with CO_2 lasers [4]. In such a high laser field intensity, the laser-atom interaction cannot be neglected, and our numerical simulation [37] predicted that the light-dressing effect should appear in the LAES signals in the small scattering angle range of $\theta < 0.5°$.

In this Letter, we report the first unambiguous experimental observation of the small-angle ($\theta < 0.5°$) peak structure in the LAES signals of Xe originating from the light-dressing effect, which has not been identified experimentally for more than thirty years since the first theoretical prediction in 1984 [9]. The measurement was done using our home-built apparatus, which was improved in the present study so that the small-angle ($\theta \geq 0.1°$) LAES signals can be detected. In the observed angular distributions of one-photon LAES processes ($\Delta E = \pm\hbar\omega$) by Xe in an intense laser field ($I = 1.5 \times 10^{12}$ W/cm^2, $\lambda = 800$ nm), we found a distinct peak profile appearing at $\theta < 0.5°$. This observation that the peak profile appears in the small scattering angle range is consistent with the results of a numerical simulation based on Zon's model [38], in which the light-dressing effect is taken into account.

The schematic of the present experimental setup is shown in Fig. 1. Details of the setup are described in our previous reports [39,40] and in the Supplemental Material [7]. The output ($\lambda = 800$ nm, $P = 0.6$ mJ/pulse) of a 5 kHz Ti:sapphire laser system is focused by the combination of a cylindrical lens ($f = 10$ m) and a spherical lens ($f = 400$ mm). In order to suppress the ionization of the sample Xe gas, the laser pulse duration is stretched to 970(50) fs, so that the peak field intensity becomes $1.5(4) \times 10^{12}$ W/cm^2. The polarization direction

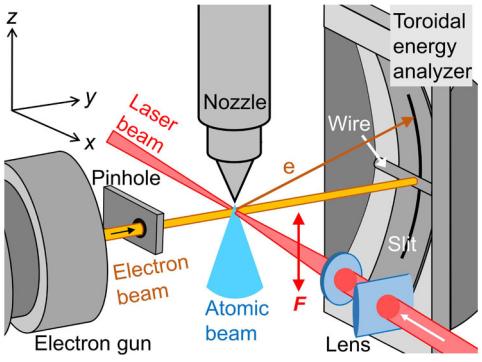

FIG. 1 (color online). Schematic of the experimental setup.

is set to be parallel to the z axis, which is "vertical" to the electron beam, where the x, y, and z axes are defined as shown in Fig. 1. An electron pulse (1000 eV) with the duration of 19(1) ps crosses both the laser beam and the effusive Xe beam at right angles 0.4 mm below the tip of the gas nozzle. Because the probability of the elastic scattering is about 1%, the contribution of the double scattering to the electron signals is estimated to be only around 1%. The kinetic energy and the scattering angle of the scattered electrons are resolved by a home-built toroidal energy analyzer [39], with which the energy resolution of 0.3 eV is achieved in the measurement of the kinetic energy shift of scattered electrons. The angular resolution is 0.24° and 0.20° for the one-photon ($\Delta E = \pm\hbar\omega$) and two-photon ($\Delta E = \pm 2\hbar\omega$) LAES processes, respectively. Electrons propagating straight without being scattered by the Xe gas are blocked by a thin Mo wire (0.35 mmφ) placed in front of the analyzer. With this setup, electrons scattered within the scattering angle range of $0.1° \leq \theta \leq 10.0°$ are detected. The background signals are measured by setting the delay time (Δt) of the electron pulse to be $\Delta t = +100$ ps. The data are accumulated 30 h for both cases of $\Delta t = 0$ ps and $\Delta t = +100$ ps.

A kinetic energy spectrum of the scattered electrons is plotted in Fig. 2(a) with red circles. The spectrum was obtained by integrating the observed electron signals over the scattering angle range of $0.1° \leq \theta \leq 10°$ and subtracting the background spectrum measured at $\Delta t = +100$ ps. In the spectrum, we observe distinct peaks centered at the energy shifts of ± 1.55 eV ($= \pm\hbar\omega$) and ± 3.10 eV ($= \pm 2\hbar\omega$). These peaks are assigned to one-photon and two-photon LAES signals, respectively. In order to confirm the assignment, we conducted a numerical simulation based on the Kroll-Watson approximation by taking into account the spatiotemporal averaging among the laser, electron, and atomic beams. Details of the simulation are described in the Supplemental Material [7]. The result of the simulation is shown by a blue solid curve in Fig. 2(a). The result of the simulation shows a good agreement with the experimental result.

In Fig. 2(b), with red circles, we show a kinetic energy spectrum of the scattered electrons detected only in the small scattering angle range of $0.1° \leq \theta \leq 0.5°$. The result of the simulation based on the Kroll-Watson approximation is also shown by a blue curve. The intensities of the observed signals at $\Delta E = \pm 1.55$ eV are 1 order of magnitude larger than those of the simulated signals. In order to confirm that the observed signals at $\Delta E = \pm 1.55$ eV are the signals originating from the LAES process, we recorded an energy spectrum of the scattered electrons by setting the laser polarization direction to be parallel to the y (horizontal) axis. At the horizontal polarization, the signal intensities of the LAES process for $|n| \geq 1$ should be suppressed significantly [36] because the electric field vector becomes nearly perpendicular to the momentum

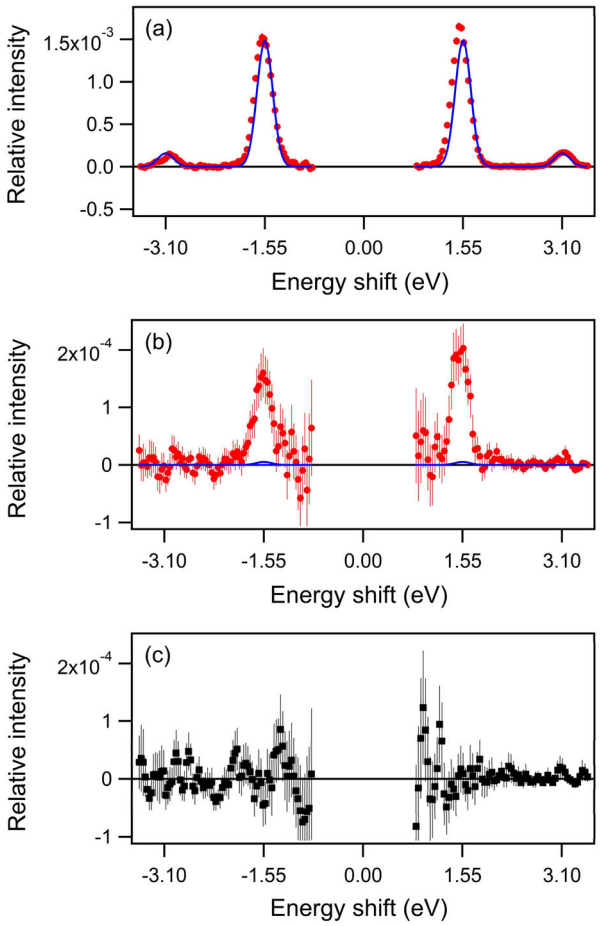

FIG. 2 (color online). The kinetic energy spectra of electrons scattered by Xe in intense laser fields obtained by the background subtraction. The signals in the range of $|\Delta E| \leq 0.8$ eV are not shown because of the large experimental errors associated with the intense background signals [36]. In (a) and (b), the energy spectra measured with the vertically polarized laser pulses are shown. Red circles show the experimental spectra. Blue lines show the spectra simulated by the Kroll-Watson approximation. These spectra are obtained by integrating the electron signals over the ranges of (a) $0.1° \leq \theta \leq 10.0°$ and (b) $0.1° \leq \theta \leq 0.5°$. (c) The energy spectrum of the scattered electrons at small scattering angles ($0.1° \leq \theta \leq 0.5°$) measured with the horizontally polarized laser pulses. All the intensities of the energy spectra are normalized by the intensities at $\Delta E = 0$ in the corresponding energy spectra before the background subtraction.

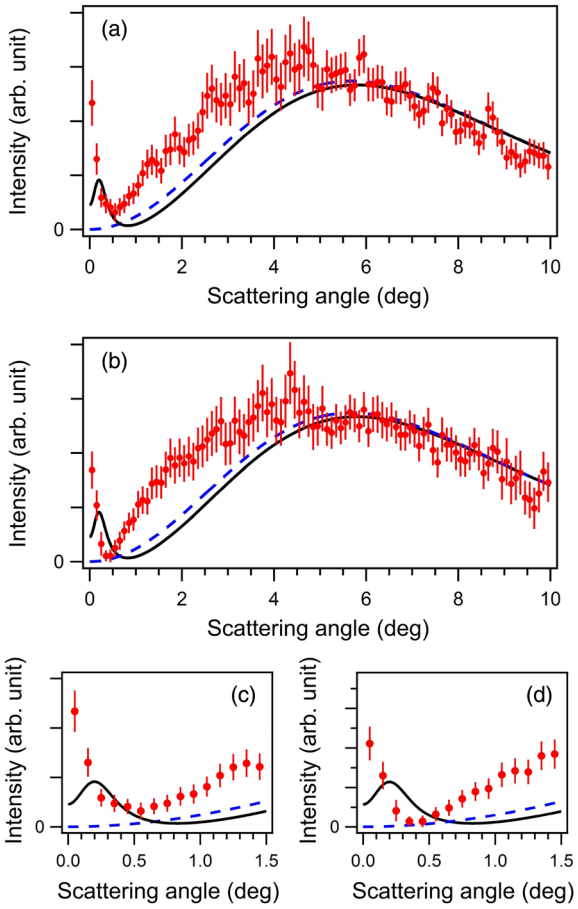

FIG. 3 (color online). The angular distributions of the LAES signals of (a) $\Delta E = +\hbar\omega$ and (b) $\Delta E = -\hbar\omega$. Red circles show the recorded angular distributions. Because of the limited angular resolution (0.24°), the angular distributions look as if the LAES signals appear even at the scattering angles of less than 0.1°. Angular distributions simulated by the Kroll-Watson approximation are shown by blue broken lines. Black solid lines are the simulated angular distributions based on Zon's model. The expanded views of the small-angle region in (a) and (b) are shown in (c) and (d), respectively.

transfer. The energy spectrum obtained after accumulating the data for 12 h with the horizontal laser polarization is shown by black squares in Fig. 2(c), which exhibits no detectable signals. This polarization dependence securely confirms that the observed signals are those originating from LAES processes.

The angular distributions of the LAES signals of $\Delta E = +\hbar\omega$ and $\Delta E = -\hbar\omega$ are shown with red circles in Figs. 3(a) and 3(b), respectively. Figures 3(c) and 3(d) are the expanded views of the small scattering angle region ($\theta < 1.5°$) of Figs. 3(a) and 3(b), respectively. These angular distributions for $\Delta E = +\hbar\omega$ and $\Delta E = -\hbar\omega$ are almost identical within the experimental uncertainties. In both of the angular distributions, a peak profile is identified at the small scattering angle range of $\theta < 0.5°$.

In order to confirm that the peak profile originates from the light-dressing effect, we also compare the experimental angular distributions with those calculated by numerical simulations. First, we show the angular distributions calculated by the Kroll-Watson approximation by blue broken lines. In the angular distributions obtained by the Kroll-Watson approximation, no peak profiles are identified at the small scattering angles. Then, we conducted a simulation in which the light-dressing effect is included according to the procedure proposed by Zon [38]. In Zon's model, the deformation of the electron density distribution of the target atom is approximately represented by a point dipole induced by the oscillating laser electric field, and

consequently, the light-dressing effect is given by the dipole-charge interaction between the laser-induced dipole and the projectile electron. The literature value of the dipole polarizability of Xe, 4.04 Å^3 [41], was used in the simulation. In Zon's model, the electron-atom interaction is treated within the first Born approximation. However, because it has been known that the first Born approximation is not good enough in evaluating the amplitude for the elastic scattering of 1 keV electrons by Xe [42], we introduced partial corrections of the higher-order Born effect into Zon's model by using the scattering amplitude of the elastic scattering without laser fields calculated by the ELSEPA package for the partial-wave analysis [43]. The modified Zon's model employed in the present study can be reduced to the Kroll-Watson approximation when the light-dressing effect is neglected by setting the dipole polarizability to be zero. Further details of the simulation based on the modified Zon's model are provided in the Supplemental Material [7]. The results of the simulation are shown in Figs. 3(a)–3(d) by black solid lines. The peaks appearing in the scattering angle range of $\theta < 0.5°$ in the simulations show that the peak profile observed at the small scattering angle can be interpreted by the light-dressing effect. On the other hand, there are discrepancies in the scattering angle range of $\theta < 0.2°$, which may be ascribed to the slight misalignment of the electron and laser beams and their pointing fluctuations during the long time accumulation. The effect of this misalignment is discussed in the Supplemental Material [7].

It can be seen in Figs. 3(a) and 3(b) that the differential cross section in the wide range of $0.5° \leq \theta \leq 5.0°$ is underestimated to a certain extent by both of the simulations based on the Kroll-Watson approximation and Zon's model, which may be ascribed to (i) the polarization of the target atom induced by the projectile electron [44], which is not included in either of the models, (ii) the point-dipole model for the target atom assumed in Zon's model, and (iii) the incomplete higher-order Born corrections in the present perturbative treatment in the modified Zon's model. Therefore, a better agreement with the experimental angular distribution will be achieved by taking into account the polarization effect and the internal structure of the deformed electron density distribution within the target atom, and by improving the corrections for the higher-order Born terms.

Finally, with the red circles in Fig. 4, we show the observed angular distribution of the LAES signals of $\Delta E = +2\hbar\omega$. This angular distribution is almost identical to that of the LAES signals of $\Delta E = -2\hbar\omega$ (not shown in Fig. 4) within the experimental uncertainties. According to the theoretical study by Beilin and Zon [45], when the electric dipole moment of a target has a component oscillating with the frequency of $n\omega$, an intense peak profile appears in the small scattering angle range in the angular distributions of the LAES signals of $\Delta E = \pm n\hbar\omega$.

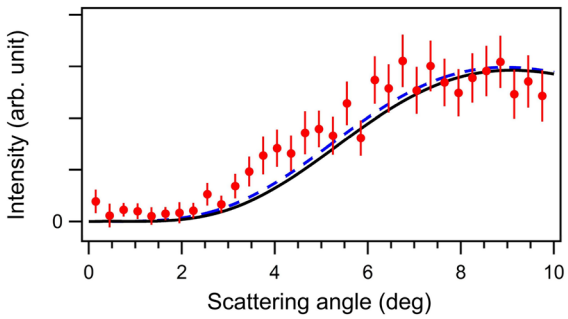

FIG. 4 (color online). The angular distribution of the LAES signals of $\Delta E = +2\hbar\omega$. The experimental angular distribution is plotted by red circles. A blue broken line and a black solid line are the simulated angular distributions obtained by the simulations based on the Kroll-Watson approximation and Zon's model, respectively.

However, because the temporal variation of the laser-induced electric dipole in an atom having originally an isotropic electron density distribution could not have even-order harmonic components [3], such an intense peak profile should not appear in the angular distribution of the LAES signals of $\Delta E = \pm 2\hbar\omega$. In fact, in the experimental angular distribution of $\Delta E = +2\hbar\omega$ shown in Fig. 4, no significant peak profile can be identified at the small scattering angle range. The experimental distribution was consistent with both of the simulations based on the Kroll-Watson approximation (broken line) and that based on Zon's model (solid line).

In summary, we have observed the light-dressing effect in the target Xe atoms in the angular distributions of the LAES signals of $\Delta E = \pm\hbar\omega$, appearing as the peak structures at $\theta < 0.5°$. The result of the numerical simulation, in which the light-dressing effect is included based on Zon's model with the effective corrections of higher-order Born terms, is consistent with the recorded angular distribution exhibiting the peak profile at $\theta < 0.5°$. Through the analysis of experimental angular distributions of the LAES signals by referring to the results obtained by more elaborate numerical simulations, we will be able to extract information on the electron density distribution within a target atom dressed by an intense laser field.

This work was supported by JSPS KAKENHI Grants No. 24245003, No. 24750011, No. 26288004, No. 24-4164, and No. 15H05696.

*kaoru@chem.s.u-tokyo.ac.jp

[1] M. H. Mittleman, *Introduction to the Theory of Laser-Atom Interactions* (Plenum, New York, 1982).
[2] F. H. M. Faisal, *Theory of Multiphoton Processes* (Plenum, New York, 1987).
[3] C. J. Joachain, N. J. Kylstra, and R. M. Potvliege, *Atoms in Intense Laser Fields* (Cambridge University Press, Cambridge, England, 2012).

[4] N. J. Mason, Laser-assisted electron-atom collisions, Rep. Prog. Phys. **56**, 1275 (1993).

[5] F. Ehlotzky, A. Jaroń, and J. Z. Kamiński, Electron-atom collisions in a laser field, Phys. Rep. **297**, 63 (1998).

[6] N. M. Kroll and K. M. Watson, Charged-particle scattering in the presence of a strong electromagnetic wave, Phys. Rev. A **8**, 804 (1973).

[7] See Supplemental Material at http://link.aps.org/supplemental/10.1103/PhysRevLett.115.123201 for details of the numerical simulations and the experimental methods.

[8] J. I. Gersten and M. H. Mittleman, Electron scattering from atoms in the presence of a laser field, Phys. Rev. A **13**, 123 (1976).

[9] F. W. Byron Jr and C. J. Joachain, Electron-atom collisions in a strong laser field, J. Phys. B **17**, L295 (1984).

[10] A. Dubois, A. Maquet, and S. Jetzke, Electron-H-atom collisions in the presence of a laser field: One-photon free-free transitions, Phys. Rev. A **34**, 1888 (1986).

[11] M. Dörr, C. J. Joachain, R. M. Potvliege, and S. Vučić, Born-Floquet theory of laser-assisted electron-atom collisions, Phys. Rev. A **49**, 4852 (1994).

[12] F. Krausz and M. Ivanov, Attosecond physics, Rev. Mod. Phys. **81**, 163 (2009).

[13] J. H. Posthumus, The dynamics of small molecules in intense laser fields, Rep. Prog. Phys. **67**, 623 (2004).

[14] D. Andrick and L. Langhans, Measurement of free-free transitions in e^--Ar scattering, J. Phys. B **9**, L459 (1976).

[15] A. Weingartshofer, J. K. Holmes, G. Caudle, E. M. Clarke, and H. Krüger, Direct Observation of Multiphoton Processes in Laser-Induced Free-Free Transitions, Phys. Rev. Lett. **39**, 269 (1977).

[16] B. Wallbank and J. K. Holmes, Laser-assisted elastic electron-atom collisions, Phys. Rev. A **48**, R2515 (1993).

[17] B. Wallbank and J. K. Holmes, Laser-assisted elastic electron-atom collisions: low electron energy and small scattering angle, J. Phys. B **27**, 1221 (1994).

[18] B. Wallbank and J. K. Holmes, Differential cross sections for laser-assisted elastic electron scattering from argon, J. Phys. B **27**, 5405 (1994).

[19] B. Wallbank and J. K. Holmes, Laser-assisted elastic electron scattering from helium, Can. J. Phys. **79**, 1237 (2001).

[20] M. O. Musa, A. MacDonald, L. Tidswell, J. Holmes, and B. Wallbank, Laser-induced free-free transitions in elastic electron scattering from CO_2, J. Phys. B **43**, 175201 (2010).

[21] I. Rabadán, L. Méndez, and A. S. Dickinson, On the validity of the soft-photon approximation for electron-atom collisions in the presence of a laser field, J. Phys. B **27**, L535 (1994).

[22] S. Geltman, Field-induced dipole effects in laser-assisted elastic electron-atom scattering, Phys. Rev. A **51**, R34 (1995).

[23] S. Varró and F. Ehlotzky, Remark on polarization effects in small angle electron scattering by helium atoms in a CO_2 laser field, Phys. Lett. A **203**, 203 (1995).

[24] C. T. Chen and F. Robicheaux, Low-energy electron-argon scattering in a low-frequency laser field, J. Phys. B **29**, 345 (1996).

[25] A. S. Dickinson, 'Small angle scattering of slow electrons by helium atoms in a CO_2 laser field: a collective model' by S. Varró and F. Ehlotzky, J. Phys. B **29**, 1569 (1996).

[26] F. Robicheaux, Collective field effects in electron-atom scattering in a low-frequency laser field, J. Phys. B **29**, 2367 (1996).

[27] N. Morrison and C. H. Greene, Laser-assisted electron-argon scattering at small angles, Phys. Rev. A **86**, 053422 (2012).

[28] I. Rabadán, L. Méndez, and A. S. Dickinson, Possible role of double scattering in electron-atom scattering in a laser field, J. Phys. B **29**, L801 (1996).

[29] D. B. Milošević and F. Ehlotzky, Off-shell low-frequency approximation for potential scattering in a laser field: comparison with the Wallbank and Holmes experiments, J. Phys. B **30**, 2999 (1997).

[30] N. J. Kylstra and C. J. Joachain, Low-energy electron-He scattering in a low-frequency laser field, Phys. Rev. A **60**, 2255 (1999).

[31] L. B. Madsen, A. Jaroń, J. Z. Kamiński, and K. Taulbjerg, Selection rule in the theory of laser-assisted charged-particle scattering. Phys. Rev. A **60**, 5126 (1999).

[32] S. Hokland and L. B. Madsen, Off-shell effects in laser-assisted scattering, Eur. Phys. J. D **29**, 209 (2004).

[33] K. M. Dunseath and M. Terao-Dunseath, Scattering of low-energy electrons by helium in a CO_2 laser field, J. Phys. B **37**, 1305 (2004).

[34] B. A. deHarak, L. Ladino, K. B. MacAdam, and N. L. S. Martin, High-energy electron-helium scattering in a Nd: YAG laser field, Phys. Rev. A **83**, 022706 (2011).

[35] B. A. deHarak, B. Nosarzewski, M. Siavashpouri, and N. L. S. Martin, Electron-helium scattering in a 1.17 eV laser field: The effect of polarization direction, Phys. Rev. A **90**, 032709 (2014).

[36] R. Kanya, Y. Morimoto, and K. Yamanouchi, Observation of Laser-Assisted Electron-Atom Scattering in Femtosecond Intense Laser Fields, Phys. Rev. Lett. **105**, 123202 (2010).

[37] R. Kanya, Y. Morimoto, and K. Yamanouchi, Laser-assisted electron scattering, and diffraction in ultrashort intense laser fields, in *Progress in Ultrafast Intense Laser Science X*, edited by K. Yamanouchi, G. G. Paulus, and D. Mathur (Springer International Publishing, Switzerland, 2014), p. 1.

[38] B. A. Zon, Bremsstrahlung in collisions between electrons and atoms, Sov. Phys. JETP **46**, 65 (1977).

[39] R. Kanya, Y. Morimoto, and K. Yamanouchi, Apparatus for laser-assisted electron scattering in femtosecond intense laser fields, Rev. Sci. Instrum. **82**, 123105 (2011).

[40] Y. Morimoto, R. Kanya, and K. Yamanouchi, Laser-assisted electron diffraction for femtosecond molecular imaging, J. Chem. Phys. **140**, 064201 (2014).

[41] J. K. Nagle, Atomic polarizability and electronegativity, J. Am. Chem. Soc. **112**, 4741 (1990).

[42] R. H. J. Jansen and F. J. de Heer, Absolute differential cross sections for elastic scattering of electrons by krypton and xenon, J. Phys. B **9**, 213 (1976).

[43] F. Salvat, A. Jablonski, and C. J. Powell, ELSEPA-Dirac partial-wave calculation of elastic scattering of electrons and positrons by atoms, positive ions and molecules, Comput. Phys. Commun. **165**, 157 (2005).

[44] M. H. Mittleman and K. M. Watson, Scattering of charged particles by neutral atoms, Phys. Rev. **113**, 198 (1959).

[45] E. L. Beilin and B. A. Zon, On the sum rule for multiphoton bremsstrahlung, J. Phys. B **16**, L159 (1983).